Spin dynamics in the $La_{1.85}Sr_{0.15}Cu_{1-x}Fe_xO_4$ system probed by ESR

Marta Z. Cieplak
Institute of Physics, Polish Academy of Sciences, 02 668 Warsaw, Poland
and Department of Physics and Astronomy, Rutgers University, Piscataway, New Jersey 08855

A. Sienkiewicz
Institute of Physics, Polish Academy of Sciences, 02 668 Warsaw, Poland

F. Mila and S. Guha
Department of Physics, Rutgers University, Piscataway, New Jersey 08855

Gang Xiao
Physics Department, Brown University, Providence, Rhode Island 02912

J. Q. Xiao and C. L. Chien
Department of Physics and Astronomy, The Johns Hopkins University, Baltimore, Maryland 21218
(Received 5 April 1993)

We study the magnetic properties of the $La_{1.85}Sr_{0.15}Cu_{1-x}Fe_xO_4$ system ($x = 0$–0.1) in the vicinity of the metal-insulator (MI) transition using static susceptibility measurements and the electron-spin resonance (ESR) of the Fe ions. Spin-glass (SG) freezing is present for all nonsuperconducting specimens. The iron ESR line broadens on approaching the freezing temperature, similarly to the effect observed in canonical spin glasses. This broadening can be attributed to the influence of the slowing down of spin fluctuations on the spin-spin relaxation rate. It depends differently on x on the two different sides of the MI transition suggesting the existence of two different SG phases: insulating (ISG) where the Fe spins couple to the Cu-spin array by superexchange interactions, and metallic (MSG), where there exists, in addition, Ruderman-Kittel-Kasuya-Yosida-like coupling mediated by the free carriers. The proximity of the MI transition suppresses this coupling, giving rise to the observed dependence of the paramagnet-SG phase boundary on x. In the MSG phase, at high temperatures, the spin-lattice relaxation mechanism is also mediated by the free carriers. It differs from the analogous process observed in conventional metals in that the ESR linewidth increases with increasing T faster than linearly. We explain this behavior by assuming that the effective magnetic field felt by the Fe moments originates mainly from the spins of holes located on the nearest-neighbor oxygen ions. The linewidth divided by T which probes the dynamical susceptibility at the Fe site varies as $a + bT$. Here a goes to zero as the MI transition is approached and so plays the role of the Pauli susceptibility of the free carriers, whereas b is independent of x in the vicinity of the MI transition but decreases for small Fe dopings away from the MI transition and may be identified as originating from the antiferromagnetic spin fluctuations in the system.

I. INTRODUCTION

A large number of recent studies has been devoted to the investigation of the nature of magnetism in the high-T_c oxides and the possible connection between superconductivity and magnetism. The spin dynamics and the mobility of free carriers in these materials are strongly interdependent. The changes in the magnetic properties are accompanied by evolution from insulating to metallic and superconducting phases. Inelastic neutron scattering provides information about the antiferromagnetic (AF) long-range order of the insulating parent compounds and the way they evolve upon doping with small amounts of free carriers.[1,2] While in the electron-doped materials doping leads to a dilution of the magnetically coupled lattice of copper spins and a decrease of the spin stiffness constant,[2] hole doping in the $La_{2-x}Sr_xCuO_4$ system gives rise to an unusual spin-glass (SG) behavior in which the spin stiffness constant is not affected, but the long-range AF order breaks down into small domains.[1] The doped holes are presumed to contribute to the creation of effective ferromagnetic coupling between Cu spins, leading to frustration in the long-range AF order.[3] At high doping levels, which give rise to superconductivity, neutron-scattering experiments are difficult to perform, as a result of strong softening and damping of spin excitations. Hence other experimental techniques need to be exploited to complement the data on spin dynamics in the metallic phase of the high-T_c oxides.

The method of probing magnetism in the CuO_2 planes which we use is to alter the Cu-spin array by introducing magnetic moments different from that of the host Cu mo-

ment, i.e., by substitution of Cu by other transition-metal elements. An example is the doping of the CuO_2 plane with Zn, which has a completely filled $3d$ shell and therefore creates a spin vacancy leading to dilution of the Cu-spin system.[4,1] A surprising but not yet well-understood effect, which has received great attention, is the very efficient suppresion of superconductivity by such vacancy doping. In the $La_{1.85}Sr_{0.15}CuO_4$ (LSCO) system doped with Zn we have found that the suppression of superconductivity is accompanied by the creation of an effective magnetic moment.[4] This is also true for other nonmagnetic impurities in LSCO (Ga and Co) (Refs. 5 and 6) and points to the complex nature of these systems.

In this study we direct our attention to the effects of doping of the Cu-spin array by large localized magnetic moments. As an impurity we use Fe, which is known to substitute for Cu in LSCO in the valence state of +3 and which retains its large magnetic moment of $S = 5/2$.[6]

The effects of magnetic impurities on high-T_c superconductivity appear to generate less interest than the effects of vacancy doping since there is nothing surprising in superconductivity being suppressed by magnetic ions. Indeed, studies of the suppression of T_c by various impurities in LSCO show that Fe affects T_c the most: T_c goes to zero at an impurity level x_c of only 1.8 at.%, whereas other trivalent impurities without a magnetic moment (Co and Ga) show a complete suppression of superconductivity at values of x_c of about 2.5 at.%.[6] However, T_c depends linearly on the Fe content, which is not consistent with the behavior found for the long-lived local moments in conventional superconductors.[7] This indicates that the effect of Fe doping might be more complex then merely the introduction of the local moments.

Intuitively one might expect that a local moment placed in an array of frustrated AF couplings should enhance spin correlations. In the presence of strong coupling between spin excitations and free carriers this should, in turn, enhance localization effects. We have recently made a thorough study of the transport properties of LSCO doped with five transition-metal impurities including Fe.[8] Among the various impurities Fe shows the strongest effect on low-T conductivity, inducing a $\sqrt{T}$ dependence of the conductivity up to surprisigly high temperatures ($\approx$ 70 K). For impurities with smaller values of the magnetic moment the $\sqrt{T}$ dependence persists to lower temperatures. Interestingly, however, this effect of spin dynamics on the transport seems to be confined to the temperature dependence of the conductivity. The critical concentration x_{MI} of the impurity at which the metal-insulator (MI) transition takes place, defined as the impurity content below which the normal-state conductivity is finite as T goes to zero, does not correlate with the effective magnetic moment. Instead, it correlates with the change in the concentration of the free carriers induced by doping (as inferred from Hall-effect measurements[9]) and the doping-induced disorder, so that x_{MI} is smallest (and similar) for the three trivalent impurities (Fe, Co, and Ga).

In order to shed additional light on the complex interplay between the magnetism and the approach to the MI transition we have performed measurements of electron-spin resonance (ESR) and of the static susceptibility for the $La_{1.85}Sr_{0.15}Cu_{1-x}Fe_xO_4$ (LSCFO) system with $0 \geq x \geq 0.1$. In all nonsuperconducting specimens we find evidence of SG freezing. The linewidth of the single ESR line from Fe $S = 5/2$ spins is strongly temperature dependent and reflects two different regimes of the Fe-spin relaxation: spin-spin relaxation at low temperatures and spin-lattice relaxation at high temperatures, in close analogy to the ESR observed in the metallic canonical SG systems.[10–16]

The linewidth broadening in the spin-spin relaxation regime, related to the slowing down of spin fluctuations on approaching the SG freezing temperature, scales differently with x on the two different sides of the MI transition. The spin-lattice relaxation is present in the metallic samples only. Based on these results we propose that two different SG phases exist, a metallic spin-glass (MSG) phase and an insulating spin-glass (ISG) phase. While Fe spins couple to the Cu-spin array via superexchange interactions in the ISG phase, in the MSG phase there exists, in addition, coupling mediated by free carriers, presumably of the Ruderman-Kittel-Kasuya-Yosida (RKKY) type. The strength of this coupling decreases in the vicinity of the MI transition. In Fig. 1 we show the phase diagram for the LSCFO system. The boundaries between the superconducting, metallic, and insulating phases are based on data published previously.[6,8] The MSG and ISG phases are the metallic and insulating

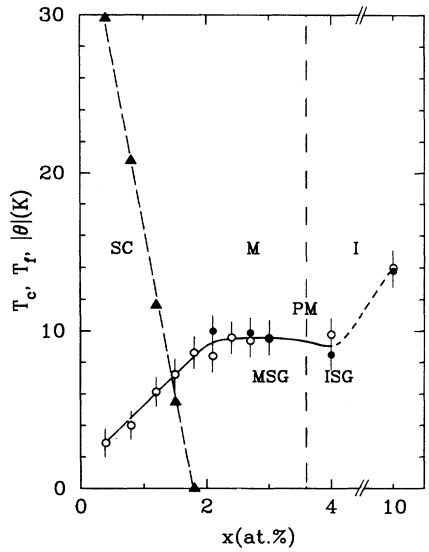

FIG. 1. Phase diagram for the $La_{1.85}Sr_{0.15}Cu_{1-x}Fe_xO_4$ system. Note the discontinuity in the scale between $x = 4$ at.% and $x = 10$ at.%. Solid triangles, open circles, and solid circles denote measured values of the superconducting transition temperature T_c, the Curie-Weiss temperature $|\Theta|$, and the spin-glass freezing temperature T_f, respectively. The dashed vertical line is drawn at x_{MI}, the critical concentration at which the MI transition occurs. SC, M, I, and PM denote the superconducting, metallic, insulating, and paramagnetic phases, respectively. MSG and ISG are the metallic and insulating spin-glass phases, as inferred from the present experiment.

spin-glass phases as inferred from the current experiment.

Despite some analogy to the canonical spin glasses, the ESR linewidth in the spin-lattice relaxation regime in the MSG phase increases with increasing temperature faster than linearly. This is different from the behavior observed in conventional metals.[17] The discussion of this result leads to interesting conclusions about the scaling properties of the susceptibility in the vicinity of the MI transition. In addition, we also study the effective g factor of the LSCFO system.

II. EXPERIMENT

A set of 12 ceramic samples of $La_{1.85}Sr_{0.15}Cu_{1-x}Fe_xO_4$, with x from 0 to 0.1 was prepared using the standard solid-state reaction method, as described in Ref. 5. X-ray diffraction showed all samples to consist of a single phase. The lattice parameters vary slightly and consistently with x: The lattice parameter along the c axis decreases by about 0.2% in the composition range studied, and along the a axis it increases by about 0.1%.

The static susceptibility was measured with a superconducting quantum interference device (SQUID) magnetometer in the temperature range 2–400 K. The ESR spectra were measured with a Bruker B-ER 418 spectrometer operating in the X band and equipped with an Oxford Instruments E900 helium-gas-flow system. The measurements were performed using both bulk polycrystalline materials and powdered samples. Because of the skin effect, the signals from bulk polycrystalline samples are weak and the line shape is Dysonian. We do not observe any anisotropic effects. The spectra presented below are for finely ground powder with an average grain size about 5–10 μm. The line shape is Lorentzian and symmetric throughout most of the temperature range except for very slight deviations at the lowest temperatures, as will be discussed below. We do not make any skin-effect correction since the symmetric shape indicates that the skin depth is larger than the grain size.

All the samples used in this study have also been used in the studies of low-temperature conductivity[8] and the Hall effect.[9]

III. STATIC SUSCEPTIBILITY

At high temperatures the static susceptibility of the LSCFO system obeys the Curie-Weiss law

$$\chi(T) = \chi_0(T) + \frac{N p_{\rm eff}^2 \mu_B^2}{3k_B(T-\Theta)}, \qquad (1)$$

where $\chi_0(T)$ is the background susceptibility, N is the impurity content, $p_{\rm eff}$ is the effective magnetic moment introduced by doping in units of the Bohr magneton μ_B, and Θ is the Curie-Weiss temperature. Figure 2 shows the results of the measurements of χ, together with the fits of Eq. (1) to the data. In the fitting procedure we have made some assumptions about the background susceptibility $\chi_0(T)$. It is about 10^3 times smaller than the Curie contribution so that it is difficult to find its precise

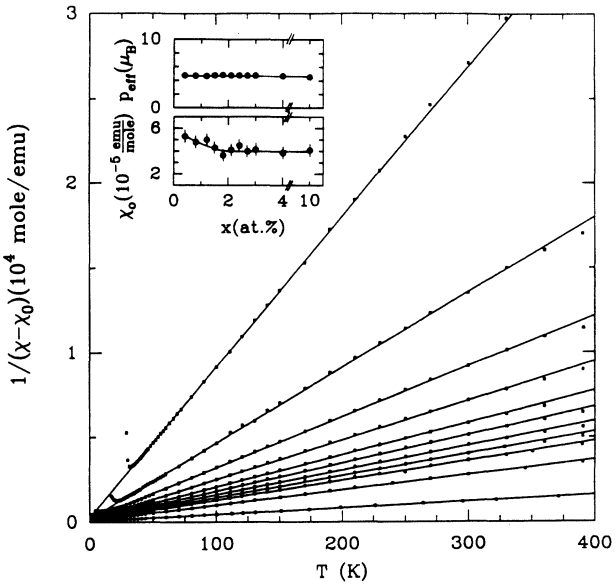

FIG. 2. The inverse susceptibility for the $La_{1.85}Sr_{0.15}Cu_{1-x}Fe_xO_4$ samples with x (from top to bottom): 0.4, 0.8, 1.2, 1.5, 1.8, 2.1, 2.4, 2.7, 3.0, 4.0, and 10 at.%. Inset: (top) the effective magnetic moment in units of the Bohr magneton, (bottom) the background susceptibility, as defined in the text.

temperature dependence. However, the data available for $La_{2-x}Sr_xCuO_4$ (Ref. 18) indicate that without the iron χ is approximately linear up to a temperature of about 200–300 K. We have therefore assumed that $\chi_0(T) = \chi_0 + \chi_1 T$ and, furthermore, that χ_1 does not change with Fe content and remains equal to the value for Fe-free LSCO. This is not precisely true, but it gives some indication of how the value of $\chi_0(T)$ at $T = 0$ changes with doping. This assumption about χ_1 leaves three parameters χ_0, Θ, and $p_{\rm eff}$, which we use in Eq. (1) to fit the experimental data.

The inset of Fig. 2 shows two parameters of the fit, $p_{\rm eff}$ and χ_0, as a function of Fe content. Within the experimental errors $p_{\rm eff}$ is constant and equal to 4.9 μ_B, consistent with the high-spin state ($S = 5/2$) of Fe^{3+} ions. The value of the parameter χ_0 has a large uncertainty. Nevertheless, it is clear that it decreases as the MI transition is approached. A similar decrease in the static susceptibility is also observed in the $La_{2-x}Sr_xCuO_4$ system when the Sr content is reduced[18] and in the $YBa_2Cu_3O_{7-\delta}$ (YBCO) system when the O content decreases.[19]

The value of the Curie-Weiss temperature is negative, indicating the existence of short-range AF interactions. The absolute value of Θ is shown in Fig. 1 as a function of x. The magnitude of Θ increases linearly for small x, shows a saturation above $x = 2$ at.%, and increases again up to about 14 K at a doping level of 10 at.%. The initial linear increase of $|\Theta|$ with x leaves no doubt that the Curie contribution to the susceptibility originates in the Fe impurities.

The solid circles in Fig. 1 are the spin-glass freezing temperatures T_f obtained from low-field (20 G) magnetization measurements. Below T_f irreversible magnetic

behavior occurs, the details of which will be presented in a future publication.[20] For the samples for which they are measured the values of T_f follow the behavior observed for $|\Theta|$ quite closely. This indicates that SG freezing is intimately related to Fe doping. While our experiment does not access the superconducting state directly, the sizable value of $|\Theta|$ in the superconducting samples suggests that SG freezing may survive even below x_c.

There are several ways in which Fe doping may induce magnetic ordering in LSCO. One of them is the reduction of the concentration of free carriers by the trivalent impurity leading to the MI transition. This should remove, or substantially reduce, the frustration of the AF Cu-Cu couplings which is present in the pure LSCO system.[1] The Mössbauer spectrum for LSCO doped with 10 at. % of Fe is analogous to the spectra observed in the parent insulating La_2CuO_4 and may indicate that the ordering is driven by Cu-Cu superexchange interactions.[21] This is likely to be true for the insulating samples. In addition, the random replacement of the Cu spins by Fe spins should modify the spin stiffness constant. The Fe-doping level is probably still too small to allow an efficient short-range Fe-Fe interaction.

The situation is quite different for the metallic samples where the change in the concentration of free carriers is still very small. Here the free carriers fully contribute to the frustration of the AF Cu-Cu couplings. The sizable value of T_f suggests that SG freezing may be driven by the interactions of Fe moments. Even small doping may introduce long-range RKKY-like exchange interactions between the Fe spins mediated by the free carriers, as commonly observed for metallic alloys.[22]

A possible effect is nonuniform localization induced by doping. Since Fe impurities are trivalent, the doping may create a nonuniform distribution of charge and thus contribute to the formation of regions in which the concentration of free carriers is reduced and the spin correlations are enhanced. In effect, Fe impurities may become centers of small domains in which the Cu spins may be AF aligned over short distances. Whatever is the detailed origin of the SG freezing, it is clear that the freezing is related to the interaction of Fe moments with the free carriers so that the SG phases on the insulating and the metallic sides of the transition are qualitatively different. As we show below this conclusion is further confirmed by the results of the ESR measurements.

IV. ESR SPECTRA

Figure 3 shows the temperature evolution of a representative ESR (derivative) spectrum measured for the sample doped with 2.7 at. % Fe. A resonance line with a g factor close to 2 is visible in a narrow temperature range, with a maximum amplitude and minimum width close to 40.5 K. The resonance field is unchanged at high temperatures, but at $T = 22.7$ K the line is shifted toward lower fields. The shape of the line remains Lorentzian at all temperatures, with the A/B ratios throughout most of the temperature range close to 4.0, the value for an ideal Lorentzian shape.[23] The largest deviation from the Lorentzian shape is observed for the lowest temperature,

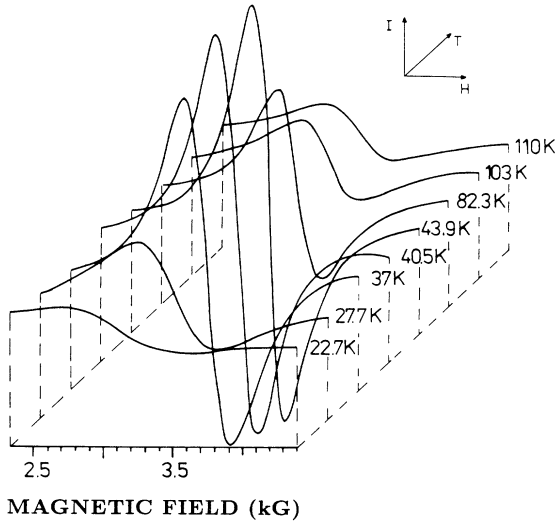

FIG. 3. ESR spectra of the sample with 2.7 at. % Fe at various temperatures.

where the A/B ratio drops to about 3.85. This value is still much larger then the value expected for a Gaussian shape (2.2), and we conclude that the contribution to the linewidth from inhomogeneous broadening is negligibly small.

The intensity and width of the resonance line depend sensitively on the Fe content, and we therefore assign this line to the isolated Fe moments. We have calibrated the intensity with the Bruker standard. The resulting number of spins per sample agrees well with the nominal Fe content.

Aside from the major resonance due to the Fe^{3+} moments, we also observe two very weak resonances centered at $g = 2.07$ and at $g = 4.18$ in some of the samples. These spectra disappear completely above $T = 25$ K and are not affected by a change in Fe content. In fact, we have observed similar low-T spectra for LSCO doped with Zn so that these resonances are clearly not related to the iron. The low-T lines are probably caused by a tiny amount of some spurious phase containing the isolated Cu^{2+} moments. After a long annealing of the samples at low temperature the low-T resonances decrease in intensity or vanish completely, whereas the Fe^{3+} signal does not change.

The temperature dependence of the effective g factor is shown in Fig. 4 for three samples with Fe contents of 0.4, 0.8, and 2.7 at. %. A sharp increase of g occurs at low temperature for the two samples with larger impurity content. The increase cannot be seen for the 0.4-at. % sample because it becomes superconducting at 30 K. At higher temperatures the effective g factor is constant within the experimental accuracy. An average value of g obtained for the high-temperature region is plotted versus Fe content in the inset of Fig. 4. The g factor for the free Fe^{3+} ion, g_{FI}, is equal to 2.0023.[24] The sample doped with the smallest amount of Fe exhibits an effective g very close to this value. The correction to this free-ion value of the g factor is negative and increases

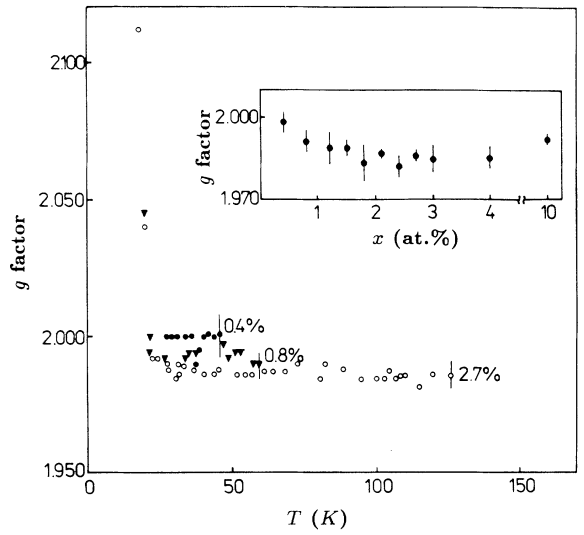

FIG. 4. Temperature dependence of the effective g factor for samples with 0.4, 0.8, and 2.7 at. % Fe. Inset: high-temperature value of the g factor versus x.

with impurity content.

The temperature dependence of the peak-to-peak linewidth ($\Delta H_{\text{p.p.}}$) is shown in Fig. 5 for samples doped with different amounts of Fe impurity. For every sample a characteristic increase of $\Delta H_{\text{p.p.}}$ is present both in the high- and the low-temperature regions. The broadening of the resonance line depends differently on the impurity content x in the low-T and in the high-T regions. This is illustrated in the inset of Fig. 5, where we show the dependence of $\Delta H_{\text{p.p.}}$ on x for two fixed temperatures, 20 K and 105 K. We see that at low temperatures the line broadens progressively as x increases, up to about 2 at. %, and then remains constant up to 4 at. %. A large increase of $\Delta H_{\text{p.p.}}$ is again observed for the sample with

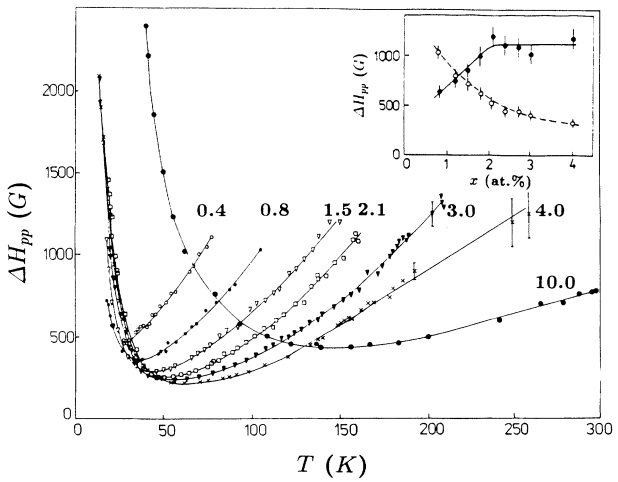

FIG. 5. Temperature dependence of the ESR linewidth for samples with various x. Inset: $\Delta H_{\text{p.p.}}$ vs x for $T = 20$ K (solid circles) and $T = 105$ K (open circles). The lines are guides to the eye.

10 at. % of Fe.

This low-T dependence of $\Delta H_{\text{p.p.}}$ on x mimics that of the spin-glass freezing temperature T_f (or Curie-Weiss temperature Θ) shown in Fig. 1. This indicates that the low-T broadening of the ESR line is intimately related to the spin-glass freezing. Taken together with the apparent increase of the g factor in the same temperature range, the ESR line broadening is analogous to that of the ESR resonance in canonical spin glasses such as *Cu*Mn,[10] *Ag*Mn,[11–13] *Au*Mn,[14] and *Au*Fe,[15] along with rare-earth spin glasses such as, for example, (*La*Gd)Al_2.[16]

The broadening of the ESR linewidth in the vicinity of T_f in spin glasses has been attributed to the modification of the spin-spin relaxation rate by the slowing down of spin fluctuations on approaching T_f.[10–13] In the paramagnetic regime at temperatures above T_f and in the absence of any other relaxation mechanism the width of the resonance line is determined by the competition between the exchange narrowing and the broadening resulting from the anisotropy of spin-spin interactions. As spin fluctuations slow down in the vicinity of T_f the narrowing becomes less effective and the width of the resonance line increases. In the absence of any significant inhomogeneous broadening in our samples the low-T increase of $\Delta H_{\text{p.p.}}$ may be attributed to this phenomenon.

We note that observation of the broadening of the ESR line does not imply that a phase transition occurs at T_f. In fact, the LSCFO system might behave similarly to LSCO where the neutron-scattering experiments fail to observe any divergence of the correlation length at low temperatures.[1] However, the ESR experiment probes the local environment on a time scale shorter then ω^{-1}, where ω is the resonance frequency. Therefore slowing down of the spin fluctuations on approaching T_f results in linewidth broadening independently of whether T_f marks a true phase transition or not.

In the high-T region the dependence of $\Delta H_{\text{p.p.}}$ on x is distinctly different from the low-T behavior (see inset of Fig. 5). The resonance line narrows as x grows. This is a consequence of the fact that in metals the spin-spin relaxation ceases to be a dominant relaxation mechanism at high temperatures. It is replaced by the spin-lattice relaxation.[17] In many cases this relaxation is mediated by the free carriers which interact through an exchange interaction with the local magnetic moments of the magnetic impurities. This should be the case for Fe^{+3} impurities for which the orbital moment of the impurity is quenched so that the direct relaxation between the local moment and the lattice is ineffective. The approach to the MI transition has a dramatic effect on the relaxation mechanism mediated by the free carriers. As the impurity content increases, the relaxation via free carriers becomes slower, thus leading to a narrowing of the ESR line.

In the following we discuss the observed spin-spin and spin-lattice relaxation mechanisms in the LSCFO system in greater detail.

V. LOW-T REGION: SPIN-SPIN RELAXATION

The increase in the ESR linewidth on approaching T_f has been previously fitted to a power law of reduced

temperature $t = (T - T_f)/T_f$.[10–12] If there is a phase transition at T_f, one expects that the characteristic time of the transverse spin fluctuations will behave critically and follow a power law. However, application of power-law scaling to our experimental data must be done with caution for at least two reasons. First, we do not find independent proof of a phase transition at T_f. Second, ESR is a local, finite-time probe, which involves the use of high magnetic fields that may affect the characteristic time of the spin fluctuations. The high magnetic fields are probably responsible for the fact that in the canonical spin glasses power-law scaling with t is observed only in a limited range of t.[11–13] The quantitative theoretical analysis of ESR experiments is complicated, and has so far not been done completely. Keeping in mind these precautions we proceed nevertheless to show that power-law scaling with t applies to the present case, albeit in a limited range of t. While we cannot give a detailed interpretation of our data in the absence of any viable theory, we nevertheless show that the scaling analysis leads to qualitative information about the spin-spin interactions in the LSCFO system.

Following Refs. 10–12 we express the low-T values of the linewidth $\Delta H_{\mathrm{p.p.}}$ as a function of t as

$$\Delta H_{\mathrm{p.p.}} = c(x)t^{-\gamma}, \tag{2}$$

where we use the values of T_f shown in Fig. 1 for all the samples for which they have been measured, and the values of the Curie-Weiss constant $|\Theta|$ instead of T_f for the rest of the samples. The coefficient $c(x)$ depends on the type and strength of the exchange interactions and on the anisotropies. In Fig. 6 we show that the quantity $\Delta H_{\mathrm{p.p.}}/c$ is a universal function of t, for t between 0.8 and 6, for all of the samples. The high-temperature deviation from linearity is caused by the spin-lattice relaxation mechanism. The deviation from linearity for $t < 0.8$ is commonly observed in spin glasses when the temperature approches T_f and its origin is a subject of debate.[11,12] We do not attempt to study this low-t range since in our experiment the values of $\Delta H_{\mathrm{p.p.}}$ for $t < 0.8$ are at least one order of magnitude larger than the ones discussed in Refs. 11 and 12 and the low-t range is not accesible for most of the samples.

The values of the exponent γ and the coefficient c are shown in Fig. 7 as a function of x. It is seen that the exponent is constant, with an average value equal to 1.3. This is very close to the value of the exponent measured for the spin glass AgMn.[11] The coefficient c, on the other hand, depends strongly on the Fe content, with a minimum at around $x = 3$ at. %. This corresponds approximately to the value of x at the MI transition, as shown by the vertical dashed line in Fig. 7. It is plausible that this dependence of c on x indicates that quite different Fe-spin interactions are present on the metallic and insulating sides of the transition, denoted in Fig. 7 as MSG (metallic spin glass) and ISG (insulating spin glass). To emphasize this difference we show in Fig. 8 a log-log plot of $c(x)$ versus T_f. The points for all metallic samples (solid circles) lie along a straight line with slope -1.3, i.e., $c = c_M T_f^{-1.3}$, where c_M is a constant. Incorporating this into Eq. (2) we see that the scaling relation for the ESR linewidth in the MSG phase is $\Delta H_{\mathrm{p.p.}} = c_M(T - T_f)^{-1.3}$. In the MSG phase the whole dependence on x of the ESR line broadening is confined to the T_f dependence on x. On the other hand, in the ISG phase $c(x)$ is an increasing function of T_f as shown by the open circles in Fig.

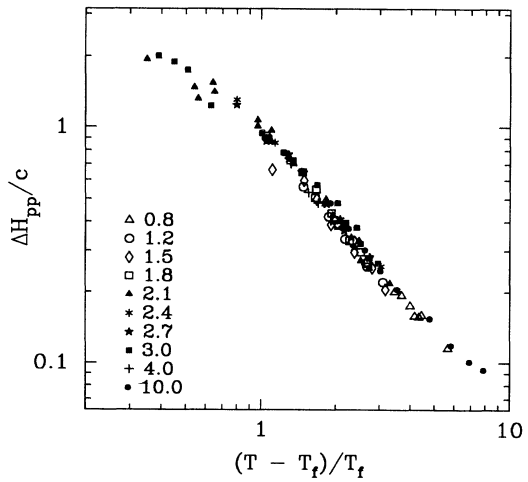

FIG. 6. Log-log plot of $\Delta H_{\mathrm{p.p.}}/c$ in the low-T region vs $t = (T - T_f)/T_f$.

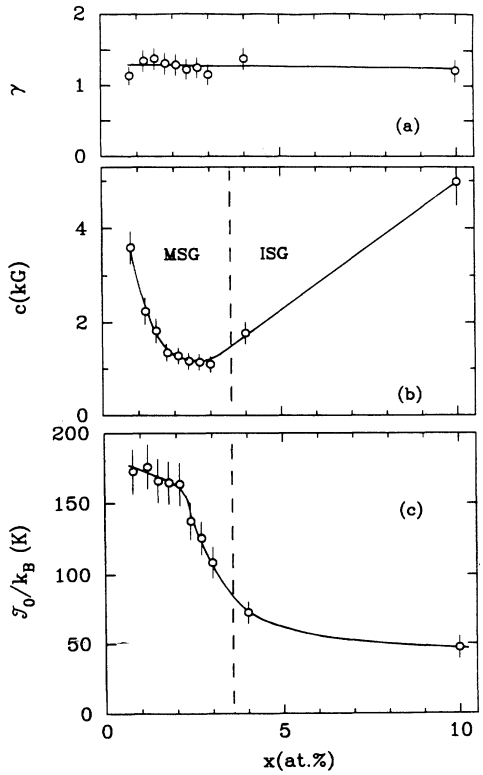

FIG. 7. Parameters of the scaling equation (2) (a) the exponent γ and (b) the coefficient $c(x)$, as a function of x. (c) The magnitude of the average exchange constant at the Fe site, $\mathcal{J}_0$, vs x.

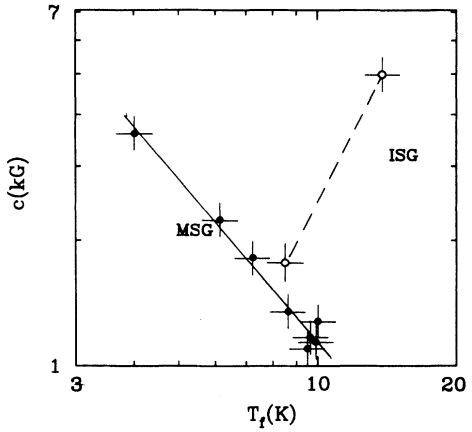

FIG. 8. Log-log plot of the coefficient c vs T_f for metallic samples (solid circles) and insulating samples (open circles). The slope of the continuous line is equal to -1.29.

8. There are too few samples to specify this function. Nevertheless, the difference between the MSG and ISG samples is quite obvious and supports the conclusion of the importance of free carriers for the interactions of Fe spins in the MSG phase.

In Fig. 7(c) we plot the values of the average exchange interaction at the Fe site, defined by the equation $\mathcal{J}_0 = 3k_B|\Theta|/xS(S+1)$. In this figure the dashed vertical line again indicates the MI transition. The value of $\mathcal{J}_0$ is equal to 175 K at small Fe dopings, but reduces as the MI transition is approached. If RKKY-like exchange interactions are responsible for the large value of $\mathcal{J}_0$ in the MSG phase, then the decrease of $\mathcal{J}_0$ with doping in the vicinity of the MI transition is caused by a reduction of the concentration of free carriers. It is interesting that $\mathcal{J}_0$ is almost constant for very small dopings (less than 2 at. %) and that the significant drop in $\mathcal{J}_0$ coincides with the transition from the superconducting to the metallic, nonsuperconducting phase. On the insulating side $\mathcal{J}_0$ reaches a value of only about a third of that observed in the metal. Once all the carriers are localized, the Fe spins are coupled to Cu neighbors by superexchange interactions only, and $\mathcal{J}_0$ again reaches a constant value. We see that the assumption of RKKY-like interactions in the MSG phase explains both the behavior of Θ and the difference in the spin-spin relaxation rate detected by the ESR on the two sides of the MI transition.

VI. HIGH-T REGION: SPIN-LATTICE RELAXATION

A. ESR linewidth

The spin-lattice relaxation via free carriers is a two-step process with two characteristic relaxation times.[17] Depending on the relative magnitude of these two times one usually observes in conventional metals either the so-called "bottleneck" regime or the "isothermal" regime. The characteristic features of the bottleneck regime are that the effective relaxation rate is proportional to the temperature but inversely proportional to the impurity content. As a result the temperature derivative of the ESR linewidth, $\frac{d(\Delta H_{\text{p.p.}})}{dT}$, increases sharply with decreasing impurity content. In the isothermal case the effective relaxation rate is linearly dependent on temperature, with both the slope and the zero-temperature intercept independent of impurity content, but proportional to the square of the density of states and to the square of the s-d exchange constant. The intercept is proportional to $-\Theta$ (the Curie-Weiss temperature), so that it is negative for positive Θ, i.e., for ferromagnetic exchange coupling.

An inspection of our experimental results shows that the dependence of $\Delta H_{\text{p.p.}}$ on temperature and impurity content cannot be described within the framework of either regime. Specifically, the dependence of $\Delta H_{\text{p.p.}}$ on T is nonlinear, as shown in Fig. 5. Even if we try to fit a straight line to a portion of the data, the slope of this line is not strongly dependent on x, contrary to the usual situation in the bottleneck regime. A straight-line fit leads to a negative value for $\Delta H_{\text{p.p.}}$ at T=0. This could be explained in the isothermal regime with a positive Θ, but the value that we observe is negative.

It is perhaps not surprising that the ESR results cannot be interpreted by the theory of conventional metals. NMR experiments in high-T_c materials also give highly unconventional results because of the strong coupling between free carriers and the antiferromagnetically coupled background in the CuO_2 planes. AF spin correlations are found to be important for the proper description of both the NMR relaxation rates and the Knight shift.[19,25–27] To understand the ESR results we adopt the approach used to interpret the NMR experiments.

We assume that the linewidth, proportional to the relaxation rate, is given by

$$\Delta H_{\text{p.p.}} \sim \int d\tau \exp(i\omega_0\tau)\,\langle \mathbf{H}(\tau)\cdot\mathbf{H}(0)\rangle, \tag{3}$$

where

$$\mathbf{H} = \mathbf{H}_0 + \mathbf{H}_1, \tag{4}$$

ω_0 is the frequency of the resonance, $\mathbf{H}_0$ is the external field, and $\mathbf{H}$ is the magnetic field felt by the Fe spin such that the effective spin Hamiltonian $\mathcal{H}$ is given by

$$\mathcal{H} = g\mu_B \mathbf{S}_{\text{Fe}}\cdot\mathbf{H}. \tag{5}$$

We assume further that the Fe spin is coupled to its nearest Cu and O neighbors only:

$$\mathcal{H} = g\mu_B \mathbf{S}_{\text{Fe}}\cdot\mathbf{H}_0 + \mathcal{J}_{\text{O}}\sum_{i=1}^{4}\mathbf{S}_{\text{Fe}}\cdot\mathbf{S}_{\text{O}\,i} + \mathcal{J}_{\text{Cu}}\sum_{i=1}^{4}\mathbf{S}_{\text{Fe}}\cdot\mathbf{S}_{\text{Cu}\,i}, \tag{6}$$

with $\mathbf{S}_{\text{O}\,i} = p^{\dagger}_{i\sigma}\boldsymbol{\sigma}_{\sigma\sigma'}p_{i\sigma'}$ and $\mathbf{S}_{\text{Cu}\,i} = d^{\dagger}_{i\sigma}\boldsymbol{\sigma}_{\sigma\sigma'}d_{i\sigma'}$, where $\boldsymbol{\sigma}$ are the Pauli matrices, and $p^{\dagger}$, $d^{\dagger}$ (p, d) are operators that create (destroy) a hole in the O $2p$, Cu $3d$ orbitals.

$\mathcal{J}_{\text{O}}$ and $\mathcal{J}_{\text{Cu}}$ are the exchange integrals resulting from kinetic exchange and superexchange, respectively. Assuming that the hopping parameter ι between Cu and O is smaller than the other characteristic energy $\mathcal{E}$ (on-site repulsions or on-site energy differences) one can show that $\mathcal{J}_{\text{O}}$ is of the order of $\iota^2/\mathcal{E}$ whereas $\mathcal{J}_{\text{Cu}}$ is of the order

of $\iota^4/\mathcal{E}^3$, so that $\mathcal{J}_O \gg \mathcal{J}_{Cu}$. Therefore, to a first approximation, the field "felt" by the Fe moments is created by the oxygen spins,

$$\mathbf{H} \approx \mathbf{H}_0 + \frac{\mathcal{J}_O}{g\mu_B} \sum_{i=1}^{4} \mathbf{S}_{O\,i}. \tag{7}$$

This expression indicates that $\Delta H_{p.p.}$, as measured by ESR, probes the dynamical spin susceptibility felt by the Fe moments, which is very close to the susceptibility felt by the nuclear spin on the O site measured in NMR experiments. There are some small differences due to the nondiagonal terms $\langle \mathbf{S}_{O\,i}\mathbf{S}_{O\,j}\rangle$ $(i \neq j)$, which should not produce any qualitative change.

We can check the validity of this reasoning by calculating $\Delta H_{p.p.}/T$, i.e., the quantity which should be comparable to $1/(T_1T)$ as measured by NMR. In Fig. 9 we show the temperature dependence of $\Delta H_{p.p.}/T$ for various values of x. The rapid increase of $\Delta H_{p.p.}/T$ at low temperatures is a result of the spin-spin relaxation mechanism as discussed earlier. In the high-T region in which the ESR linewidth is given by the spin-lattice relaxation rate, $\Delta H_{p.p.}/T$ can be described by the linear function

$$\frac{\Delta H_{p.p.}}{T} = a + bT, \tag{8}$$

with both the parameters a and b dependent on x, but in a different fashion as shown in the inset of Fig. 9. The parameter a decreases gradually with x and approaches zero at the MI transition. In contrast, b is only weakly dependent on x, and decreases slightly with decreasing x in the region of small x. The description given by Eq. (8) is valid for the metallic samples only, i.e., for Fe contents smaller than 4 at. %. In the insulating sample (10 at. %) there is no spin-lattice relaxation.

A comparison of Fig. 9 to the NMR results of Alloul, Ohno, and Mendals[19] on ^{89}Y sites shows a qualitative similarity between the two sets of data. $1/(T_1T)$ has been found to be temperature independent only in $YBa_2Cu_3O_7$. For all the samples with smaller amounts of oxygen, $1/(T_1T)$ decreases when the temperature is lowered. In the temperature range in which the ESR experiment was performed $1/(T_1T)$ displays an approximately linear dependence on T. Similar results have been obtained by Takigawa *et al.*[26] for the NMR relaxation rate measured on the ^{17}O site in $YBa_2Cu_3O_{6.63}$.

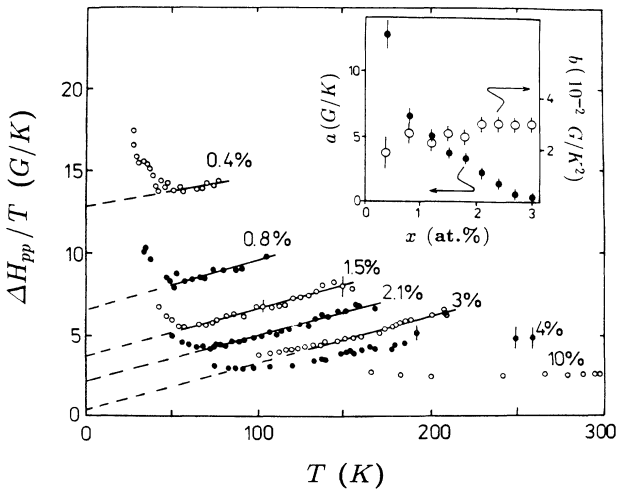

FIG. 9. Temperature dependence of $\Delta H_{p.p.}/T$ for various values of x. The solid lines represent least-squares fits of the linear function $a + bT$ through the high-temperature data. Inset: a (solid circles) and b (open circles) vs x.

Since $\Delta H_{p.p.}/T$ probes the spin susceptibility "felt" by Fe moments, one may predict that Eq. (8) may cease to be valid if one increases the Sr content above 25 at. % so that $La_{1.75}Sr_{0.25}CuO_4$ becomes a normal metal. Indeed, a qualitative change in the behavior of the ESR linewidth for large Sr dopings has been observed by Onoda and Sato,[28] although they did not study the effect quantitatively.

Equation (8) suggests that at least in the limited temperature range of our measurements one can divide the total susceptibility into two parts. The temperature-independent part a dissapears at the MI transition and therefore plays the role of a Pauli susceptibility of free carriers. The remaining T-dependent part may then be associated with the AF spin fluctuations. This part remains relatively constant as a function of x in the vicinity of the MI transition, and decreases only for small doping levels, suggesting that the role of the spin fluctuactions diminishes as one goes away from the MI transition.

It is evident from Fig. 9 that the decrease of a is not linear with increasing x. It is useful to examine the dependence of a on the distance to the MI transition, defined as $x_{MI} - x$, where x_{MI} is the critical concentration at which the MI transition takes place. Our low-temperature conductivity measurements[8] lead to a scaling law for the zero-T conductivity, $\sigma_0 \sim (x_{MI} - x)^{\nu}$, with x_{MI} equal to 3.6 at. % Fe and a critical exponent ν equal to 1. This exponent is commonly observed at the MI transition in homogeneous metal-nonmetal mixtures in which disorder is present on the atomic length scale. The exponent of one is consistent with the predictions of the scaling theory for the interaction-driven MI transition for the case of strong spin-flip scattering in the presence of long-range interactions.[29] In Fig. 10 we show a log-log plot of a and σ_0 versus $(x_{MI} - x)/x_{MI}$. A least-squares fit gives a critical exponent for a equal to 2.07 ± 0.2. In other words, the parameter a scales to zero with an exponent twice as large as for the conductivity.

To complete the picture of the scaling properties it would be interesting to know the scaling exponent for the static susceptibility in our samples and how it is related to a. Unfortunately, this is difficult because of the large Curie-Weiss term in the static susceptibility. We can, however, at least compare a and the χ_0 part of the susceptibility which was defined in Sec. III and shown in Fig. 2. This comparison is presented in Fig. 11(a). It is evident that a decreases with decreasing χ_0 as the insulating phase is approached. The large uncertainty of χ_0 prevents us from finding the exact functional relation between a and χ_0.

There are various possibilities for the difference in the critical exponents of the relaxation rate and the conduc-

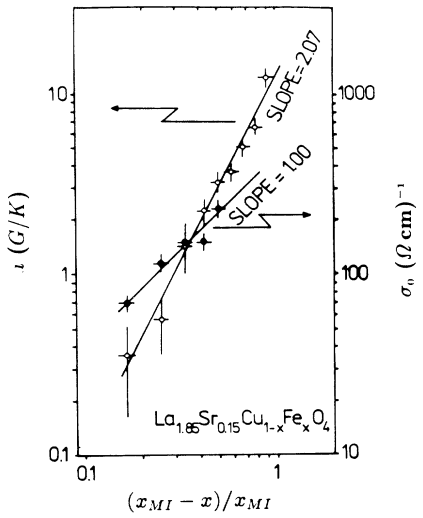

FIG. 10. Dependence of a and σ_0 on $(x_{\rm MI}-x)/x_{\rm MI}$. The least-squares fits give scaling exponents for a and σ_0 equal to 2.07 and 1.00, respectively.

tivity. In a conventional metal the spin-lattice relaxation rate is proportional to the square of the Pauli susceptibility. One interesting possibility is that this relation holds also in the present case so that the scaling exponent of the susceptibility is 1. On the other hand, the scaling exponents of the conductivity, the susceptibility, and the relaxation rate may be quite different from one another in the vicinity of the MI transition. In fact, the studies of Si:P (Ref. 30) indicate a difference between the temperature dependence of the macroscopic susceptibility and the local susceptibility probed by the Knight shift. The results are interpreted in terms of inhomogeneous spin localization. For the present MI transition one can imagine that localization effects might be enhanced in the vicinity of an impurity. Then $\Delta H_{\rm p.p.}/T$, which probes the strictly local environment of the impurity, would "feel" localization effects more strongly than the conductivity, which is an average property of the sample. This would be quite reasonable since the Fe impurity has a valence of 3+ and may therefore attract a negative charge. On the basis of the present experiment we cannot decide which one of the above explanations is appropriate. It would be interesting to determine whether the difference in the scaling exponents is a property of this specific MI transition caused by the substitution of Fe ions into Cu sites or is a more general feature present in other high-T_c oxides. We are planning further experiments to investigate this question.

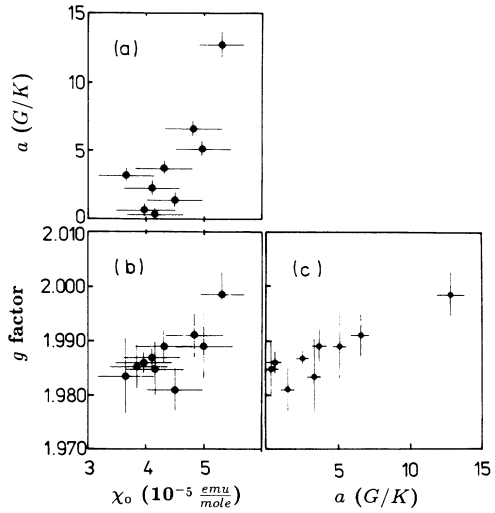

FIG. 11. (a) The coefficient a as a function of χ_0. (b) The g factor as a function of χ_0. (c) The g factor as a function of the coefficient a.

B. Effective g factor

So far we have discussed only the relaxation rates. Another quantity measured in our experiment is the effective g factor. As shown in the inset of Fig. 4 the g factor is close to the free-ion value $g_{\rm FI}=2.0023$ for small x and decreases when the insulating phase is approached. The comparison of the g factor to the static susceptibility χ_0 and to the intercept a is presented in Figs. 11(b) and 11(c). From Fig. 11(c) we find $g_{\rm in}$, the g factor in the insulating phase at $a=0$, to be 1.984 ($\pm$0.001). Despite the large error bars, it is clear from Fig. 11(b) that the decrease in χ_0 correlates with the decrease of the g factor. Therefore at least part of the deviation of the g factor from the free-ion value is the result of the coupling of the Fe moments to their O neighbors. Hence the effective g factor may be expressed as

$$g_{\rm eff}=g_{\rm FI}+\delta g+\Delta g, \tag{9}$$

where Δg is due to the Fe-O coupling and δg represents all the other deviations not related to this coupling. In the insulating phase there are no holes in the O orbitals so that $\Delta g\to 0$ when $g_{\rm eff}\to g_{\rm in}$. It follows that $g_{\rm in}=g_{\rm FI}+\delta g$ and $\delta g<0$. The deviation of $g_{\rm in}$ from the free-ion value results from corrections not related to the Fe-O interaction. In the presence of free carriers a positive Δg must be added, bringing the effective g factor nearly to the free-ion value. The sources of the correction unrelated to the Fe-O coupling may include, for example, the spin-orbit coupling which, in the case of the d^5 electronic configuration, can introduce a small admixture of the excited state $^4P_{\frac{5}{2}}$ to the ground state $^6S_{\frac{5}{2}}$.[24] The resulting deviation of the g factor can in principle be of either sign, although it is negative in the present case. In most systems the corrections are small, of the order of 3×10^{-3}, but larger corrections were also observed, e.g., $g_{\rm eff}=2.019$ for Fe^{3+} in ZnS.[24]

VII. CONCLUSIONS

We have used the measurements of susceptibility and the electron-spin resonance of Fe ions to probe the magnetic properties of the LSCFO system as it is tuned, by Fe doping, through the superconductor-metal-insulator transition. SG freezing is observed for all nonsupercon-

ducting specimens. Althougth our experiment does not probe superconducting samples below T_c directly, the sizable value of the Curie-Weiss temperature suggests that SG freezing may survive also in the superconducting regime.

In the metallic specimens the ESR reflects two different regimes of Fe-spin relaxation: the spin-spin relaxation at low temperatures and the spin-lattice relaxation at high temperatures, in analogy to the metallic canonical spin glasses. In the insulating specimens the spin-lattice relaxation is absent. The ESR linewidth broadening in the spin-spin relaxation regime originates from the slowing down of spin fluctuations on approaching the SG freezing temperature. The linewidth scales differently with the Fe content on the two different sides of the MI transition. This is consistent with the existence of two different SG phases, the metallic (MSG) and the insulating (ISG). In the ISG-phase Fe spins couple to the surrounding Cu-spin lattice via superexchange interactions. In the MSG phase there exists, in addition, the RKKY-like coupling mediated by the free carriers, which is suppressed by the proximity of the MI transition. This suppression accounts well for the dependence on x of the paramagnet spin-glass phase boundary.

The spin-lattice relaxation in the MSG is mediated through an exchange interaction of the free carriers and the Fe moments. It differs from the analogous process observed in conventional metals in that the ESR linewidth increases with increasing temperature faster than linearly. We are able to explain this dependence successfully by assuming that the effective magnetic field "felt" by the Fe moments originates mainly from the spins of the holes located on the nearest-neighbor oxygen ions. The linewidth divided by T probes the dynamical spin susceptibility at the Fe site. It depends linearly on the temperature $\Delta H_{\mathrm{p.p.}}/T = a + bT$, with the parameter a gradually decreasing to zero as the MI transition is appoached, and b only weakly x dependent, mostly in the region of small x, i.e., away from the MI transition. This result indicates that, at least in the limited temperature range in which ESR probes the spin-lattice relaxation, one can divide the susceptibility into two parts: a, the part which plays the role of a temperature-independent Pauli susceptibility of the free carriers, and bT, the part which appears to have its origin in the AF spin fluctuations of the system. We find that the scaling exponent for a is close to 2, twice as large as the scaling exponent for conductivity, as measured for the same samples. The difference in the scaling laws may indicate, among other possibilities, that a is proportional to the square of the Pauli susceptibility, as in conventional metals. The difference may also originate from inhomogeneous localization in the vicinity of the MI transition.

Finally, we would like to emphasize another possible implication of our ESR data. NMR indicates different temperature dependences of the nuclear relaxation rates measured at the ^{63}Cu sites and at ^{17}O (or ^{89}Y) sites in YBCO, which are interpreted as originating from short-range AF spin correlations, and more specifically from the vanishing of the form factor at $\mathbf{q} = (\pi, \pi)$ in the case of O or Y nuclei.[31–33] There are not enough NMR data for the $La_{2-x}Sr_xCuO_4$ system to determine whether the ^{17}O and ^{63}Cu relaxation rates in this compound behave similarly to those in YBCO. However, if the behavior is similar, the form-factor argument cannot explain the results of our experiment. We find that $\Delta H_{\mathrm{p.p.}}$ measured at the Fe sites behaves similarily to the O-site NMR relaxation rate. Since the Fe spin is at the Cu site, it is not clear why AF correlations should be filtered out at the Fe site. Therefore the currently accepted models of the relaxation rate in the presence of AF correlations seem to require some modification to be able to account for the present experiment.

ACKNOWLEDGMENTS

We would like to thank P. Lindenfeld, A. Ruckenstein, and Z. Wilamowski for valuable discussions. This work was supported by grants from the Polish Committee for Scientific Research Nos. 2-0469-9101 and 2-0470-9101, and by NSF Grants Nos. DMR 88-22559, DMR 89-17027, and DMR 90-24402.

[1] B. Keimer, N. Belk, R. J. Birgeneau, A. Cassanho, C. Y. Chen, M. Greven, M. A. Kastner, A. Aharony, Y. Endoh, R. W. Erwin, and G. Shirane, Phys. Rev. B **46**, 14034 (1992).
[2] M. Matsuda, Y. Endoh, K. Yamada, H. Kojima, I. Tanaka, R. J. Birgeneau, M. A. Kastner, and G. Shirane, Phys. Rev. B **45**, 12548 (1992).
[3] A. Aharony, R. J. Birgeneau, A. Coniglio, M. A. Kastner, and H. E. Stanley, Phys. Rev. Lett. **60**, 1330 (1988).
[4] G. Xiao, M. Z. Cieplak, and C. L. Chien, Phys. Rev. B **42**, 240 (1990).
[5] M. Z. Cieplak, G. Xiao, A. Bakhshai, and C. L. Chien, Phys. Rev. B **39**, 4222 (1989).
[6] G. Xiao, M. Z. Cieplak, J. Q. Xiao, and C. L. Chien, Phys. Rev. B **42**, 8752 (1990).
[7] M. B. Maple, Appl. Phys. **9**, 179 (1976).
[8] M. Z. Cieplak, S. Guha, H. Kojima, P. Lindenfeld, G. Xiao, J. Q. Xiao, and C. L. Chien, Phys. Rev. B **46**, 5536 (1992).
[9] G. Xiao, P. Xiong, and M. Z. Cieplak, Phys. Rev. B **46**, 8687 (1992).
[10] M. B. Salamon and R. M. Herman, Phys. Rev. Lett. **41**, 1506 (1978); M. B. Salamon, Solid State Commun. **31**, 781 (1979).
[11] G. Mazurkewich, J. H. Elliott, M. Hardiman, and R. Orbach, Phys. Rev. B **29**, 278 (1984).
[12] W. Wu, G. Mazurkewich, and R. Orbach, Phys. Rev. B **31**, 4557 (1985).
[13] H. Mahdjour, C. Pappa, R. Wendler, and K. Baberschke, Z. Phys. B **63**, 351 (1986).
[14] D. Varknin, D. Davidov, G. J. Nieuwenhuys, F. R. Hoekstra, G. E. Barberis, and J. A. Mydosh, Physica **108B**, 765 (1981).
[15] B. R. Coles, B. V. B. Sarkissian, and R. H. Taylor, Philos. Mag. B **37**, 489 (1978).
[16] M. Zomack, K. Baberschke, and S. E. Barnes, Phys. Rev.

B **37**, 4135 (1983).
[17]S. E. Barnes, Adv. Phys. **30**, 801 (1981).
[18]D. C. Johnston, Phys. Rev. Lett. **62**, 957 (1989).
[19]H. Alloul, T. Ohno, and P. Mendels, Phys. Rev. Lett. **63**, 1700 (1989); J. Less-Common Met. **164-165**, 1022 (1990).
[20]J. Q. Xiao *et al.* (unpublished).
[21]I. Felner, U. Yaron, I. Nowik, and E. R. Bauminger, Physica C **198**, 14 (1992).
[22]K. Binder, Rev. Mod. Phys. **58**, 801 (1986).
[23]R. S. Alger, *Electron Paramagnetic Resonance: Techniques and Applications* (Wiley, New York, 1968), p. 43.
[24]A. Abragam and B. Bleaney, *Electron Paramagnetic Resonance of Transition Ions* (Dover, New York, 1986).
[25]R. E. Walstedt, W. W. Warren, Jr., R. F. Bell, G. F. Brennert, G. P. Espinoza, R. J. Cava, L. F. Schneemeyer, and J. V. Waszczak, Phys. Rev. B **38**, 9299 (1988).
[26]M. Takigawa, A. P. Reyes, P. C. Hammel, J. D. Thompson, R. H. Heffner, Z. Fisk, and K. C. Ott, Phys. Rev. B **43**, 247 (1991).
[27]H. Yasuoka, T. Imai, and T. Shimizu, in *Strong Correlation and Superconductivity*, edited by H. Fukuyama, S. Maekawa, and A. P. Malozemoff (Springer, Berlin, 1989); W.W. Warren, Jr., Phys. Rev. Lett. **62**, 1193 (1989).
[28]M. Onoda and M. Sato, Solid State Commun. **70**, 309 (1989).
[29]P. A. Lee and T. V. Ramakrishnan, Rev. Mod. Phys. **57**, 287 (1985); C. Castellani, C. DiCastro, P. A. Lee, and M. Ma, Phys. Rev. B **30**, 527 (1984).
[30]H. Alloul and P. Dellouve, Phys. Rev. Lett. **59**, 578 (1987).
[31]F. Mila and T. M. Rice, Phys. Rev. B **40**, 11382 (1989).
[32]P. C. Hammel, M. Takigawa, R. H. Heffner, Z. Fisk, and K. C. Ott, Phys. Rev. Lett. **63**, 1992 (1989).
[33]B. S. Shastry, Phys. Rev. Lett. **63**, 1288 (1989).